ELSEVIER

Contents lists available at ScienceDirect

Environmental Pollution

journal homepage: www.elsevier.com/locate/envpol





Surface-modified biopolymers for removing mixtures of per- and polyfluoroalkyl substances from water: Screening and removal mechanisms*

Aswin Kumar Ilango ^{a,*}, Tao Jiang ^a, Weilan Zhang ^a, Jeremy I. Feldblyum ^b, Haralabos Efstathiadis ^c, Yanna Liang ^a

- a Department of Environmental and Sustainable Engineering, University at Albany, State University of New York, Albany, NY, 12222, United States
- b Department of Chemistry, University at Albany, State University of New York, Albany, NY, 12222, United States
- ^c College of Nanoscale Science and Engineering, SUNY Polytechnic Institute, Albany, NY, 12203, United States

ARTICLE INFO

Keywords: Per- and polyfluoroalkyl substances Bio-based fibers and aerogels Biosorbent's screening Adsorption pH Isotherms

ABSTRACT

Green, renewable, and sustainable materials are needed for removing per- and polyfluoroalkyl substances (PFASs) in water. Herein, we synthesized and tested alginate (ALG) and chitosan (CTN) based and polyethyleneimine (PEI) functionalized fibers/aerogels for the adsorption of mixtures of 12 PFASs (9 short- and long-chain PFAAs, GenX, and 2 precursors) from water at an initial concentration of 10 μ g/L each. Out of 11 biosorbents, ALGPEI-3 and GTH CTNPEI aerogels had the best sorption performance. Through detailed characterization of the sorbents before and after PFASs sorption, it was revealed that hydrophobic interaction was the dominant mechanism controlling PFASs sorption while electrostatic interactions played a minor role. As a result, both aerogels had fast and superior sorption of relatively hydrophobic PFASs from pH 2 to 10. Even at extreme pH conditions, the aerogels retained their shape perfectly. Based upon the isotherms, the maximum adsorption capacity of ALGPEI-3 and GTH-CTNPEI aerogels towards total PFASs removal was 3045 and 12,133 mg/g, respectively. Although the sorption performance of the GTH-CTNPEI aerogel toward short chain PFAS was less than satisfactory and varied between 70 and 90% in 24 h, it may find its use in removing relatively hydrophobic PFAS at high concentrations in complex and extreme environments.

1. Introduction

Per- and polyfluoroalkyl substances (PFASs) are a wide group of environmentally persistent organic compounds of industrial origin and have been of great concern globally due to their toxicity and bio-accumulation (Lindstrom et al., 2011). The PFASs family is made up of compounds having different chain lengths of carbon-fluorine (C–F) and different functional groups, such as carboxylic or sulfonic acids attached at one end. (Saleh et al., 2019), (Zhang et al., 2021) PFASs possess extreme chemical/thermal stabilities due to their strong C–F bonds, which makes them highly persistent in the aquatic environment (Yao et al., 2014). The U.S. EPA recently published the interim lifetime health advisory levels of PFOA and PFOS in drinking water as 0.004 ng/L and 0.02 ng/L, respectively (Rabinow, 2022). These extremely low levels pose a serious challenge to remediation and demand innovative and

sustainable technologies to remove PFASs in water to such low concentrations (Stratton et al., 2017).

Conventional treatment processes, such as biological treatment (Arvaniti and Stasinakis, 2015), oxidation (Finnegan et al., 2018), disinfection by chlorine or UV irradiation (Appleman et al., 2014), (Rahman et al., 2014) have been demonstrated to be ineffective for PFASs removal. PFASs removal by adsorption (Liu et al., 2016), however, is an established technology, both as a single process for point-of-use applications and as an unit operation in the process of treating water at municipal scale (Carter and Farrell, 2010). As of now, numerous adsorbents have been synthesized, assessed, and reported in the literature for PFASs removal. Among them, a few are commercially available, such as granular activated carbon (GAC) (McCleaf et al., 2017), powdered activated carbon (PAC) (Chen et al., 2017), clay (Luft et al., 2022), and resin (Zaggia et al., 2016) etc., Among these few, GAC

 $[\]ensuremath{^{\star}}$ This paper has been recommended for acceptance by Jiayin Dai.

^{*} Corresponding author.1400 Washington Avenue, Albany, NY, 12222, United States. *E-mail address:* ailango@albany.edu (A.K. Ilango).

has been used broadly. But GAC is known to have slow adsorption kinetics and much lower efficiency in removing short-chain PFASs and precursors than long-chain ones (Saha et al., 2021). In addition to these technical limitations, a large fraction of GAC on the market is made from coal through either physical or chemical processes demanding high temperatures (400–1200 °C) (Kopac et al., 2017) and/or the use of harmful and toxic chemicals.

Newly developed sorbents, such as modified clay or organoclay have exhibited much higher sorption capacity and faster kinetics than those of GAC. (Jiang et al., 2022), (Mukhopadhyay et al., 2021) These organoclays, however, are often in powdered form that gives them large specific surface area for sorption. These powders, once in water, may form stable colloids which are difficult to remove from water. The powder particles themselves also necessitate centrifugation or filtration for separation. These drawbacks thus may hinder their application in real-world drinking water treatment (Oladipo and Gazi, 2014).

Biopolymers, such as chitosan (CTN) and alginate (ALG) are natural polysaccharides extracted from the exoskeleton of crustaceans and cell walls of brown algae, respectively. (Tan et al., 2008; Kumar et al., 2021), (Pandi and Viswanathan, 2015), These biopolymers possess advantages, such as being biocompatible, biodegradable, nontoxic, inexpensive, and broadly available. To improve the adsorption performance of biopolymers, the reactive functional groups present in CTN and ALG, such as –NH2 and –OH, can be chemically modified through cross-linking, functionalization, etc. (Ahmad et al., 2017), (Jiang et al., 2013) Polyethyleneimine (PEI) is a water-soluble polymer with repeating units composed of abundant -NH2 and two carbon aliphatic -CH2-CH2- spacers (Yan et al. 2019). Sufficient protonation of the -NH2 to –NH3 under acidic conditions leads to immobilization of anions through electrostatic attractions (Lu et al., 2020). Moreover, the cross-linking of PEI onto biopolymers enhances their structural stability (Yan et al., 2017a).

In recent years, few studies have reported the use of biosorbents for removing PFASs in water. As discussed in later sections, most of these biosorbents are amine-modified natural materials used in powdered form (Li et al., 2022), (Zhang et al., 2019), (Hassan et al., 2022) to remove only PFOA or PFOS at mg/L levels. These mg/L concentrations are seldomly observed in the environment. Although high sorption capacities have been reported, it is questionable whether these sorbents can achieve complete removal of PFASs mixtures containing these compounds with different chain length, functional groups, structures and at µg/L or ng/L concentrations.

Hence, in this study, we sought to synthesize and screen ALG- and CTN- based biosorbents. The best sorbents were expected to have high sorption capacity toward mixtures of 12 PFASs (Table S1) and possess fast sorption kinetics, excellent shape recovery, and structural stability. The top-performing sorbents were then investigated further to understand the mechanisms underlying the sorption performance. Studying representative PFASs mixtures at environmentally relevant concentrations adds significant insights to the practical use of the target sorbents for removing PFASs in a wide range of water matrices, for instance drinking water, storm water, effluent from wastewater treatment plants, and landfill leachate. These insights and knowledge will guide proper material selection and design and shorten the distance and time from laboratory studies to using these materials in the real-world for solving critical challenges related to PFASs.

2. Experimental section

2.1. Materials

The chemicals and reagents used in this study are shown in Table S2. Milli-Q water (resistivity $\geq \! 18.0~M\Omega \cdot \! cm)$ was used to prepare PFASs solutions.

2.2. Preparation of biosorbents

2.2.1. ALG/PEI (ALGPEI) based aerogel

ALGPEI based aerogel was prepared adopting the procedure reported by Wang et al., (2022) In short, 0.1 g of Na-ALG was dissolved in a mixed solution of 4.90 mL of deionized water and 0.14 mL of glutaraldehyde (GTH) (5 wt %) in a 100 mL polypropylene beaker. The solution was then stirred for 45 min to achieve a transparent ALG solution without any air bubbles. To this ALG solution, a PEI solution [0.24 mL of PEI (50% in water) + 4.90 mL of deionized water] was added dropwise for 30 min with vigorous stirring for a total of 3 h at 25 $^{\circ}$ C to reach a uniform pink emulsion. Finally, the obtained ALGPEI emulsion was incubated at 60 °C for 1 h to achieve ALGPEI gelation. The gel was then frozen at $-20~^{\circ}\text{C}$ for 24 h followed by freeze-drying at $-45~^{\circ}\text{C}$ for 24 h. The resulting ALGPEI aerogel is referred to as ALGPEI-1 throughout the rest of this paper. ALGPEI-2 and ALGPEI-3 were likewise prepared through using PEI at 0.48 and 0.97 mL, respectively. In addition, ALGPEI based fibers and cetyltrimethylammonium chloride (CTAC) surfactant modified ALGPEI (CTAC-ALGPEI) aerogels were also prepared as given in the Text S1 and Text S2 respectively, in the Supporting Information.

2.2.2. CTN/PEI (CTNPEI)-based aerogel using GTH cross-linker

The procedure for ALGPEI aerogel was also applied for the synthesis of CTNPEI based aerogel. In this case, 0.1 g of CTN was dissolved in the mixed solutions of 2% acetic acid (v/v) and GTH (5 wt %) in a 100 mL polypropylene beaker (Karthik and Meenakshi, 2015). The solution was then stirred for 30 min, after which time a PEI solution was added dropwise for 30 min, followed by additional stirring at 25 °C for 3 h. This produced a uniform brownish-orange emulsion. After incubating the emulsion at 60 °C for 1 h, the obtained gel was then frozen at $-20\,^{\circ}\text{C}$ for 24 h followed by freeze drying at $-45\,^{\circ}\text{C}$ for 24 h to obtain GTH-CTNPEI aerogel. Similarly, epichlorohydrin (ECH) cross-linked CTNPEI (ECH-CTNPEI) aerogels were prepared (Text S3) as shown in the Supporting Information.

After preparation, all biosorbents were stored in tightly sealed containers at 25 °C for further use. The images of all biosorbents synthesized in this study are shown in Fig. S1 and the weight percentages of the biopolymers, PEI, and other components of the biosorbents are listed in Table S3. The instrumental characterization of these biosorbents, PFASs sorption experiment, isotherm experiments and PFASs analysis can be found in Text S4 to Text S7 in the Supplementary Information.

3. Results and discussion

3.1. Screening of biopolymers-based fibers and aerogels for adsorption of PFASs in aqueous mixtures

3.1.1. ALGPEI fibers

As shown in Fig. S2, the removal efficiencies of the prepared fibers were found to be less than 70% for all target PFASs. Short chain PFASs removal by these fibers was even less effective despite increasing PEI to 50 wt %. The beneficial effect of PEI was only detected for four PFASs: PFDA, PFUnA, PFOS, and N-EtFOSAA. The exact PEI content leading to enhancement of PFASs sorption, however, differed among these four. For PFUnA, the highest removal was observed for those with PEI at 13 wt %. In the case of PFOS, a gradual increase of removal from ALG to ALGPEI-C was noticed, but the overall removal % of total PFASs by all ALGPEI fibers was found to be <30%.

Theoretically speaking, higher PEI content can provide more reactive –NH₂ functional groups (Wang et al., 2021b; Dangi et al., 2022; Wang et al., 2022) on the ALG surface, which should improve PFASs binding. But our study here showed that PEI's role in PFASs adsorption was insufficient, especially for PFCAs, PFBS, PFHxS, GenX and 6:2 FTSA. For the four PFASs where enhancement of sorption by PEI was observed, the dose response effects were different. This may be due to the possibility that the presence of PEI blocks the available surface binding sites of

otherwise pristine ALG, and this decrease of surface area led to different sorption behavior of different PFASs. Overall, the ALGPEI fibers were proven to be ineffective for PFASs adsorption and they were not investigated further in this study.

3.1.2. ALGPEI and CTNPEI aerogels

To identify the equilibrium time for PFASs adsorption for these aerogels, subsamples were collected at 1, 4, 8 and 24 h as shown in Fig. 1. It was observed that: (1) the ALGPEI aerogels had higher removal of all PFASs compared to ALGPEI fibers (Figs. S2 and 1); (2) for ALGPEI-1 and ALGPEI-2, PFASs removal increased with time from $1\ \text{to}\ 24\ \text{h}.$ This is true for all target PFASs; (3) regarding ALGPEI-3, the time effect was not significant. Within 1 h, this sorbent removed 100% of PFNA, PFDA, PFUnA, PFOS and 2-N-EtFOSAA and was the best among all tested sorbents for removing these five PFASs. Its removals of PFOA, PFHxS and 6:2 FTSA were close to those of GTH-CTNPEI. In terms of short chain PFASs, such as PFHxA, PFHpA, GenX, and PFBS, ALGPEI-3 was inferior to GTH-CTNPEI. Compared to ALGPEI-1 and ALGPEI-2, the structural stability of the ALGPEI-3 aerogels was significantly higher as a result of increasing the PEI dose from 28.57 to 90.91 wt %; (4) Among all sorbents assessed, GTH-CTNPEI had the best performance for removing PFHxA, PFHpA, PFOA, PFHxS, PFBS, 6:2 FTSA and GenX. Its sorption of long chain PFASs was similar to those of ALGPEI-3; and (5) the other sorbents, ECH-CTNPEI-1, ECH-CTNPEI-2, and CTAC-ALGPEI had similar sorption performance for the long chain PFASs as those of ALGPEI-3, but their captures of short chain PFASs were less than satisfactory compared to GTH-CTNPEI.

In this study, ECH and GTH were used as cross-linkers to enhance the binding nature of PEI with biopolymers. (Wang et al., 2021b), (Zhou et al., 2014) It was observed that the ECH-assisted CTNPEI aerogels had weaker structural stability than the GTH-CTNPEI aerogels (Fig. S1). Additionally, ECH cross-linker is often considered as carcinogenic in nature while GTH is not as toxic as ECH. (Waidyanatha et al., 2014),

(Negahban et al., 2014) Given the much better performance of GTH-CTNPEI for removing all PFASs, this sorbent was studied further.

Surfactants have been used to modify clay and led to organoclays for removing PFASs. (Zhou et al., 2010), (Wang et al., 2021a) Detailed studies have been reported for Fluoro-sorb and matCARE. Recently, Jiang et al. reported that CTAC-modified clays had far superior performance for removing both long and short chain PFASs in water compared to conventional sorbents, such as GAC (Jiang et al., 2023). Hence, in this study, we were interested to see whether CTAC-modified ALGPEI could remove PFASs more effectively than the unmodified material. As expected, the CTAC-ALGPEI aerogel exhibited higher adsorption than ALGPEI-3 for short chain PFASs, PFOA, GenX and 6:2 FTSA. Its adsorption of PFUnA, PFOS and 2-N-EtFOSAA, however, was less than that of ALGPEI-3. Additionally, the structural stability of ALGPEI-3 weakened due to the inclusion of CTAC into the aerogel network. Thus, the CTAC-ALGPEI-3 aerogel was not studied further.

From all screening tests conducted, ALGPEI-3 and GTH-CTNPEI aerogels were identified as the best for PFASs adsorption. Both aerogels were able to remove almost 100% of relatively hydrophobic PFCAs (C9-C11), PFOS, and 2-N-EtFOSAA in 1 h. GTH-CTNPEI was also able to remove 70-90% of the other relatively hydrophilic PFASs. To understand the time effect better, we assessed PFASs removal by these two aerogels at shorter time intervals, such as 15, 30, 45 and 60 min. It was revealed that: 1) adsorption of all target PFASs with ALGPEI-3 was spontaneous under the tested conditions. Adsorption of 100% PFCAs (C9-C11), PFOS, and 2-N-EtFOSAA was achieved in 15 min; and 2) similarly, GTH-CTNPEI aerogels exhibited immediate adsorption of these five PFASs. Its adsorption of short chain PFASs, such as PFHxA, PFHpA, PFBS, and GenX, however, did increase slightly as the contact time rose from 15 to 60 min (Fig. S3). To better understand the sorption performance/mechanisms, the effect of pH, sorption isotherms, and sorbent structures were further investigated for these two types of aerogels.

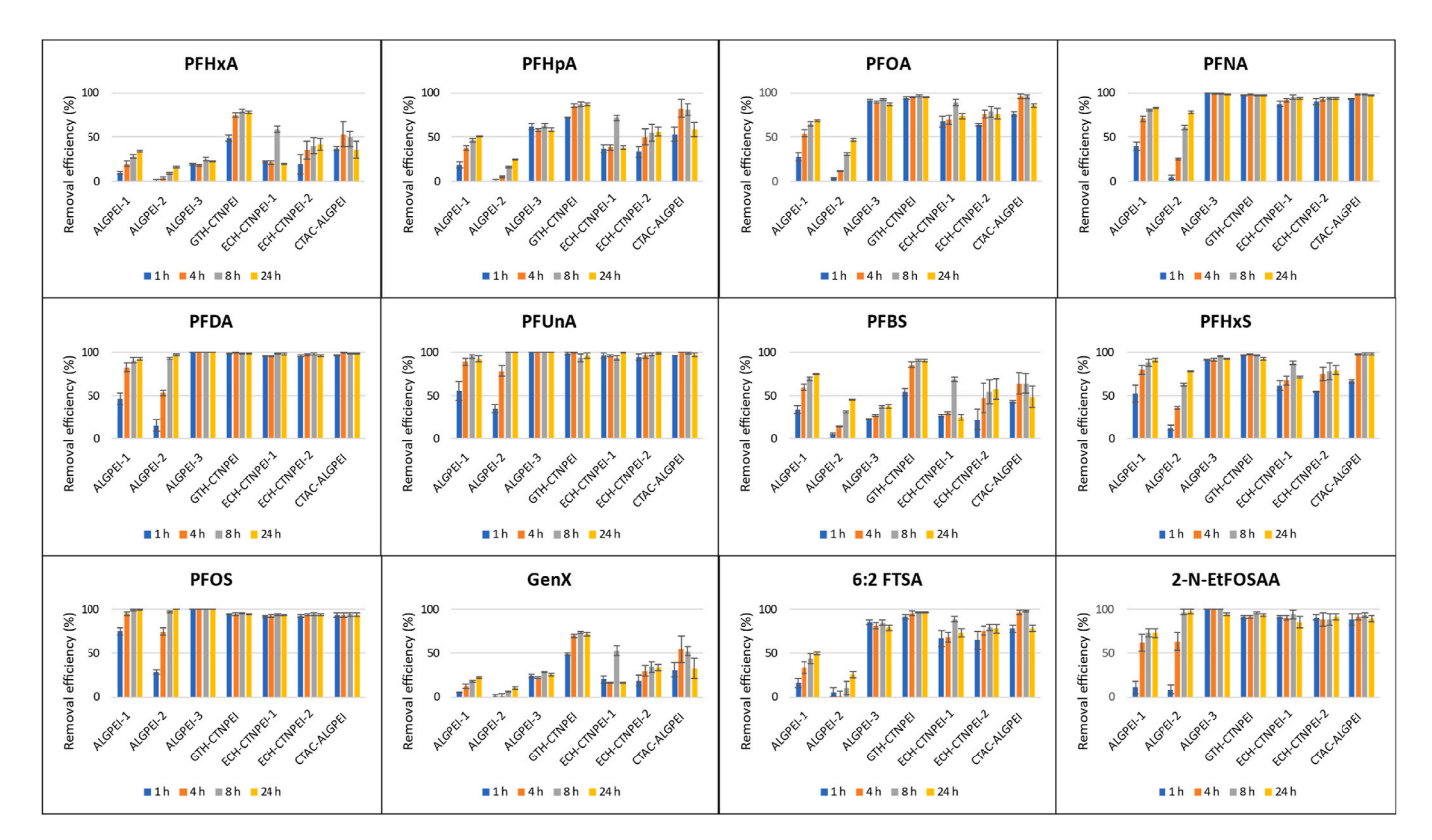


Fig. 1. Adsorption of PFASs by ALGPEI-1, ALGPEI-2, ALGPEI-3, GTH-CTNPEI, ECH-CTNPEI-1, ECH-CTNPEI-2 and CTAC-ALGPEI aerogels at 1, 4, 8 and 24 h. Initial PFASs concentration: 10 µg/L, and aerogel's dose: 100 mg/L. Error bars represent the standard deviations of triplicate measurements. Some error bars are not visible due to their small sizes.

3.2. Physiochemical characterization studies of aerogels and their adsorption mechanisms towards PFASs removal

3.2.1. FTIR investigation

FTIR was performed to verify the composition, i.e., the functional groups, in the prepared aerogels and to confirm the adsorption mechanism involved in PFASs removal. In Fig. 2A showing the FTIR spectra of all three ALGPEI aerogels, the stretching vibration of the O-H group of ALG appeared as a broad band in the range of 3303–3269 cm⁻¹ (Shan et al., 2019). The asymmetric and symmetric vibrations of the -COOfrom carbonyl and carboxyl groups of ALG were detected in the range of 1601-1589 and 1462-1403 cm⁻¹, respectively (Pan et al., 2021). The C-O-C and C-O/C=O stretching vibrations in the carboxyl component of ALG appeared in the range of 1291–1287 and 1025 cm⁻¹, respectively (Kumar and Viswanathan, 2017). In the FTIR spectra of the ALGPEI-3 aerogel, a band at 3276 cm⁻¹ showed up as one that could be attributed to the N-H stretching vibrations of PEI (with higher dose) in addition to the O-H stretching vibration of ALG (Yan et al., 2017b). The antisymmetric stretching and bending vibrations of C-H in -CH₂/-CH₃ groups of PEI was observed around 2927-2920/2807-2805 and 821-816 cm⁻¹, correspondingly (Bo et al., 2020). Essentially, the signal at 1455 cm⁻¹ was related to the stretching vibrations of N-H from PEI, whose intensity rose with increasing dose of PEI as seen in the FTIR spectra of ALGPEI-1 to ALGPEI-3, further showing that the NH2 group of PEI was successfully grafted onto ALG (Feng et al., 2021; Wang et al., 2022).

In the FTIR spectra of the GTH-CTNPEI aerogel (Fig. 2B), the wide stretching vibrations of N-H and O-H groups of CTN was observed at around 3388 cm⁻¹ (Kumar and Viswanathan, 2018). The characteristic amide I vibration, bending vibration of C-H, and stretching vibration of C-O-C were detected at around 1657, 1429, and 1100 cm⁻¹, respectively (Zhang et al., 2020). The antisymmetric stretching and bending vibrations of C-H in the -CH2/-CH3 groups of PEI were observed at 2913/2848 and 968 cm⁻¹, respectively (Bao et al., 2020). The adsorption band at 1554 cm⁻¹ was associated with the C-N asymmetric stretching vibration, which was generated by the attractive interaction between the NH2 groups from PEI and CTN, indicating that these polymers were linked through GTH (Lü et al., 2021). It was observed that most of the FTIR bands of ALGPEI-3 and GTH-CTNPEI aerogels reappeared in the FTIR spectra of those containing PFASs. Some of the bands in the original sorbents disappeared, indicating the interactions between PFASs and the aerogel's surface.

Results from the FTIR studies hinted that the PFASs adsorption mechanisms were: (i) Electrostatic interactions by -OH and -NH₂

functional groups: in the ALGPEI-3 aerogel, the broad stretching vibrations of N-H and O-H at 3269 cm⁻¹ were reduced in intensity after PFASs adsorption, whereas for the GTH-CTNPEI aerogel, the same stretching vibrations were shifted to a higher wavenumber of 3672 cm⁻¹. (Harris et al., 2022), (Xiao et al., 2012), (Wawrzkiewicz and Hubicki, 2009) This demonstrated that the electrostatic interactions did occur between the protonated functional groups (O-H and N-H) of the aerogels and anionic PFASs. (ii) Hydrophobic interactions: in the GTH-CTNPEI aerogel, the higher stretching and bending vibrations of C-H in -CH2/-CH3 groups of the PEI were observed at 2979 and 2906 cm⁻¹, respectively, after PFASs adsorption, which confirmed the dominant hydrophobic interactions between the C-H groups of PEI and C-F of PFASs. In the case of ALGPEI, the C-H bands of the PEI were also observed at 2920/2807 cm⁻¹, but were not strong compared with that in the FTIR spectra of PFASs containing GTH-CTNPEI aerogel. (Dixit et al., 2019)., (Bazri and Mohseni, 2016)

There were no specific FTIR bands detected as a result of PFASs adsorption. Zhang et al. reported that the typical FTIR band for PFOS is around $1200-1350~{\rm cm}^{-1}$, which corresponds to the vibrations of $-{\rm CF}_3$ and $-{\rm CF}_2$ - groups and could be used as an indicator of organic fluorine (Zhang et al., 2013). The other bands shown in $1150-1250~{\rm cm}^{-1}$ and $1000-1075~{\rm cm}^{-1}$ could be assigned to the vibrations of organic sulfonate (SO $_3$) group. Hence, the strong FTIR signals listed above after adsorption confirmed that PFASs molecules were strongly connected with the aerogels' surface via electrostatic and hydrophobic interactions. The interactions between PFASs and the GTH-CTNPEI aerogel were stronger than those of the ALGPEI-3 aerogel, which explains overall higher removal efficiencies of GTH-CTNPEI towards PFASs than the ALGPEI-3 aerogel.

3.2.2. SEM, EDS, and BET

Scanning electron microscopy (SEM) was used to investigate the surface morphology of the ALGPEI-3 and GTH-CTNPEI aerogels (Fig. S4). With respect to the ALGPEI-3 aerogel, the surface coating and cross-linking of 1.0 g PEI to ALG provided an uneven open honeycomblike structure. For the GTH-CTNPEI aerogel, with the PEI dose of 80 wt % to CTN of 8 wt % cross-linked using GTH of 12 wt %, the aerogel started to assemble into a more homogeneous and denser network, which possessed an ideal interconnected framework (Wang et al., 2022). It is noteworthy that there was no microporous structure of the aerogels due to the high dose of PEI (i.e., 1:10 ratio of the biopolymer and PEI). In this case, the PEI completely covered the biopolymer's surface, leading to the decrease of the porous properties of the aerogels (Wang et al., 2021b). The elemental composition in the EDS spectra (Figure S4 (C)

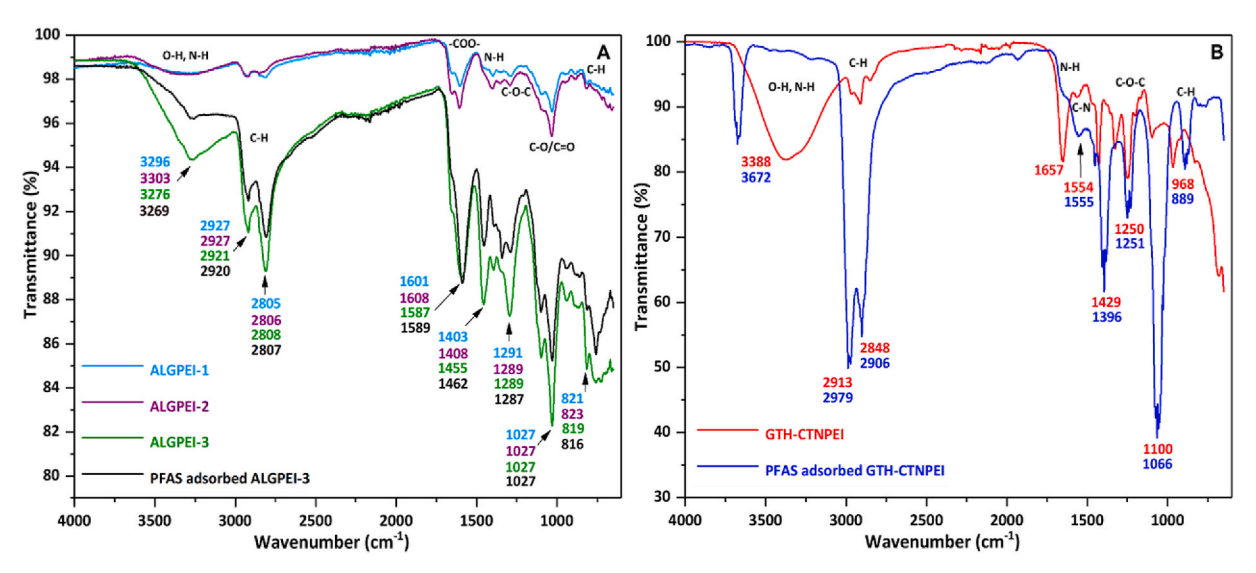


Fig. 2. FTIR spectra of (A) ALGPEI-1, ALGPEI-3 and PFASs containing ALGPEI-3, (B) GTH-CTNPEI and PFASs containing GTH-CTNPEI aerogels.

and S4 (D)) indicated that the significant elements of ALGPEI-3 and GTH-CTNPEI aerogels included C, N and O. The insignificant Na element with 0.12 wt% was from the sodium alginate biopolymer.

For analysis of pore size distribution (PSD), both aerogels were activated under the same reduced pressure (50 mTorr) condition at 25 °C for 24 h. The results are shown in Table S4. During PSD analysis, both aerogels showed extremely low absorbances, and their isotherms were hard to interpret since they were close to 0. As a result, both aerogels possessed low BET surface area and PSD. PEI at the high dose appeared to play a key role in reducing the porous surface of the aerogels (Mo et al., 2019). From SEM and PSD analysis, it was concluded that the synthesized aerogels were not porous in nature and their structural stabilities were found to be stronger with increasing dose of PEI. Therefore, the adsorption performances of the aerogels were mainly due to the amine functionalization and the –CH₂- segments of the PEI onto the biopolymers, but not the surface area and porous nature of the aerogels. (Yang et al., 2020), (Tian et al., 2021)., (Ateia et al., 2018)

3.2.3. Thermogravimetric analysis (TGA)

To assess the thermal stabilities of the ALGPEI-3 and GTH-CTNPEI aerogels, TGA was performed in the range of room temperature-700 °C (Fig. S5). The weight losses of the aerogels were divided into three stages. The first stage below 125 °C with 14.63% weight loss for ALGPEI-3 and 34.13% weight loss for the GTH-CTNPEI aerogel was due to the evaporation of water molecules (i.e., bound water and physically absorbed water) and organic solvents (GTH) on the surface of the GTH-CTNPEI aerogel (Liang et al., 2021). During the second stage at 125–223 °C, the weight loss of ALGPEI-3 was 6.24%. At 101–210 °C, the weight decrease of the GTH-CTNPEI aerogel was 17.30%. These weight reduction might be attributed to the decomposition of unstable oxygen functional moieties (Zhao et al., 2018). At the final stage, the major weight loss for both aerogels occurred. For ALGPEI-3, 71.93% of weight decrease took place from 308 to 450 °C. Regarding the GTH-CTNPEI

aerogel, 59.89% weight loss happened from 295 to 480 °C. These weight losses were due to the further decomposition of the polymer networks, i.e., CTN, ALG and PEI and cross-linked polymer chains (Li et al., 2018). Thus, it was concluded that the ALGPEI-3 aerogel could be thermally stable up to 420 °C while the GTH-CTNPEI aerogel are stable up to 480 °C. At temperatures higher than these, both aerogels became carbonaceous residues.

3.3. Effect of solution pH

The pH of a given solution alters the surface properties of a sorbent, which leads to change of adsorption performance of the sorption material (Ching et al., 2020). At the same time, the solution pH also affects the chemistry of the adsorbates, in this case, PFASs. As shown in Fig. 3, in terms of ALGPEI, pH values between 2 and 10 had no observed effect on removal of relatively hydrophobic PFASs, such as PFNA, PFDA, PFOS and 2-N-EtFOSAA. For these four PFASs, a pH value of 1.0 led to decreased removal. Specific for PFUnA, pH values between 4 and 10 had no significant effect on the removal efficiency. However, much less sorption of this PFAS was observed at pH = 1 and 2. Regarding relatively hydrophilic PFASs, for instance PFCAs (C6-C9), PFBS, PFHxS, GenX and 6:2 FTSA, pH at 4.0 appeared to result in the highest removal efficiencies. For GTH CTNPEI aerogels, the effect of pH on sorption of the five relatively hydrophobic PFASs was the same as that for ALGPEI-3. For relatively hydrophilic PFASs, the removal efficiencies at pH between 4 and 8 did not have significant differences.

A large number of PFASs has extremely low pKa (Table S2). As a result, under a wide range of pH conditions, PFASs are negatively charged (Deng et al., 2010). At acidic pH 4, the functional groups (i.e., $-NH_2$, -OH) on the aerogel's surface would be protonated, leading to enhanced electrostatic attractions between the positively charged aerogel's surface and anionic PFASs compounds in the aqueous solution (Dixit et al., 2019). Highly acidic conditions at pH = 1 and 2, however,

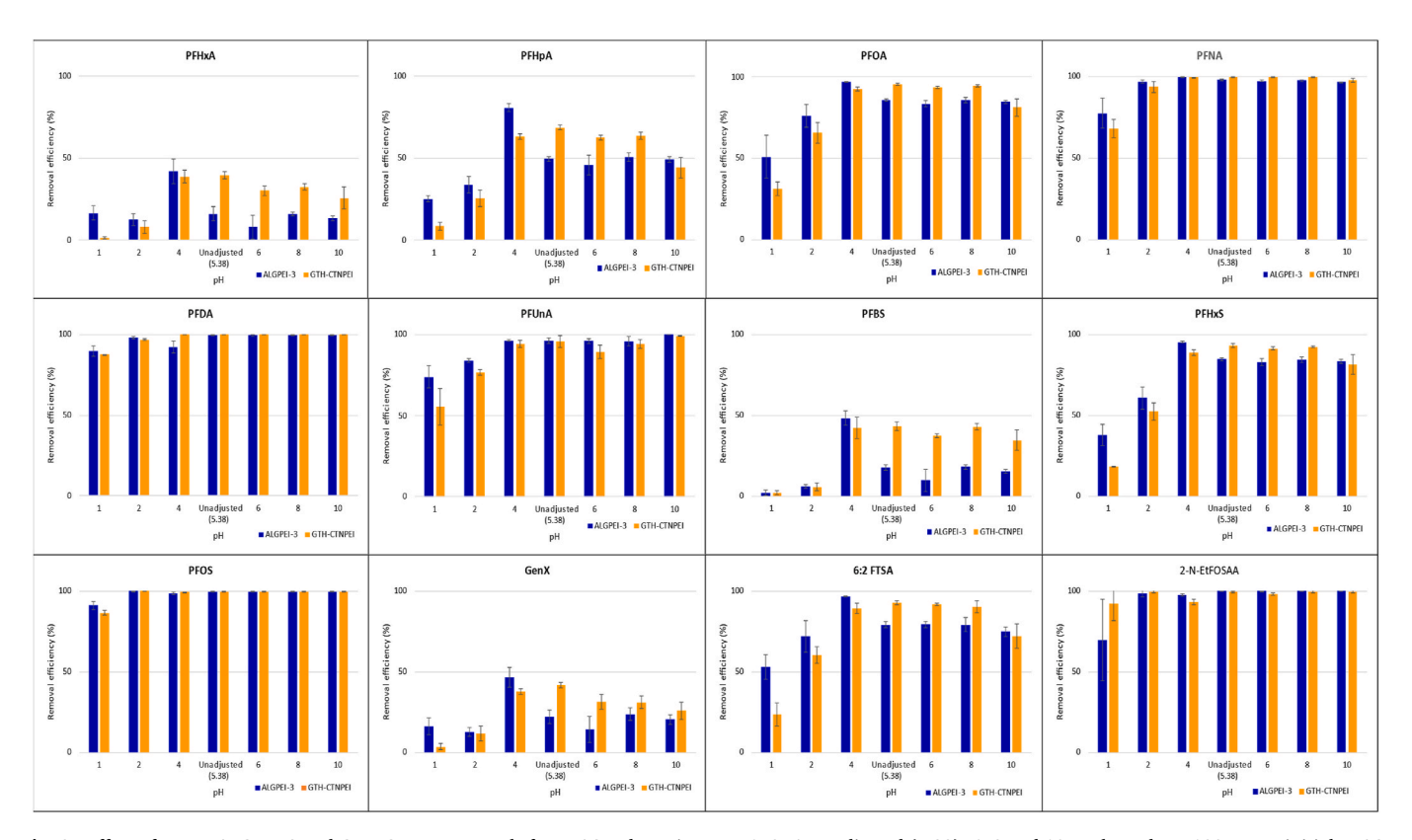


Fig. 3. Effect of pH on ALGPEI-3 and GTH-CTNPEI aerogels for PFASs adsorption. pH: 1, 2, 4, unadjusted (5.38), 6, 8 and 10; sorbent dose: 100 mg/L; initial PFASs concentration: 10 μg/L and time 1 h. Error bars represent the standard deviations of triplicate measurements. Some error bars are not visible due to their small sizes.

might result in electrostatic repulsion as both the aerogel and PFASs were highly protonated although the aerogels upheld their structural stability very well at these extremely acidic conditions. A similar result was observed by Du et al., where the removal of PFOA, PFHxA and PFHpA at pH=2 was lower than that at pH=4 (Du et al., 2015).

As pH increased to basic (pH > 7) conditions, the deprotonation of -OH and -NH₂ groups would lead to electrostatic repulsion between the adsorbent's surface and anionic PFASs compounds. This repulsion would result in decreased removal efficiencies (Higgins and Luthy, 2006). Tian et al. reported that the removal efficiency of PFOA by amino-functionalized graphene oxide (AGO) aerogel decreased from 99.9% to 89.4% with increasing pH from 1.60 to 9.26. This was assumed to be due to the formation of electronegative surface of the AGO aerogel and increased electrostatic repulsion between PFOA and the AGO aerogel at higher pH (Tian et al., 2021). But in our case, both aerogels had broad pH tolerance regarding their adsorption performance. This was especially true for GTH-CTNPEI aerogel. This clearly indicated that hydrophobic interaction was the dominant mechanism underlying PFASs adsorption under a wide range of pH (Gong et al., 2016), overcoming the electrostatic repulsions between PFASs and negatively charged adsorbent's surfaces at high pH values (Wang et al., 2019).

3.4. Isotherm studies

Three common isotherm models (i.e., Langmuir, Freundlich, Sips) were used to fit experimental adsorption data. The Langmuir isotherm considers the dynamic equilibrium of adsorption and desorption on a monolayer solid surface. The Freundlich isotherm predicts adsorption processes occurring on heterogeneous (multilayer) surfaces, while the Sips model combines the Langmuir and Freundlich isotherms and covers adsorption in heterogeneous systems (Yan et al., 2020a). As described above, both types of the aerogel had outstanding adsorption performance for long chain and relatively hydrophobic PFASs, and hence, the $C_{\rm e}$ value for individual PFASs at low initial concentrations were close to or lower than the limit of detection (LOD). To resolve this issue, the total $q_{\rm e}$ and $C_{\rm e}$ values of all tested PFAS compounds instead of individual ones were used for these isotherm models. (Tzabar and ter Brake, 2016).

As shown in Fig. S6, for both ALGPEI-3 and GTH-CTNPEI aerogels, the Freundlich model had an excellent fit in all range of PFAS concentrations. The calculated $q_{\rm e}$ from the isotherm models were compared with the experimental $q_{\rm e}$ (Table S5). The relationship between the initial concentrations (C₀) and the mass of PFASs adsorbed by ALGPEI-3 and GTH-CTNPEI aerogels were shown in Figs. S7 and S8, respectively. Based upon the Sips isotherms, the maximum adsorption capacity of ALGPEI-3 and GTH-CTNPEI aerogels towards total PFASs removal was 3045 and 12,133 mg/g, respectively (Table 1).

3.5. Adsorption capacity comparison and uniqueness of the aerogels prepared in this study

As shown in Table S6, the ALGPEI-3 and GTH-CTNPEI aerogels

Table 1Isotherm parameter values for both types of aerogels.

| Isotherm model | Parameter | Value | |
|----------------|--|---------------------|-----------------------|
| | | ALGPEI-3 | GTH-CTNPEI |
| Langmuir | R^2 | 0.99 | 0.98 |
| | $K_L (L/\mu g)$ | 1.0×10^{-4} | 5.24×10^{-5} |
| | $q_m (mg/g)$ | 202 | 6232 |
| Freundlich | R^2 | 0.99 | 0.99 |
| | $K_F (\text{mg L}^{1/m}/(\text{g }\mu\text{g}^{1/m}))$ | 0.05 | 0.03 |
| | m | 1.15 | 0.68 |
| Sips | R^2 | 0.99 | 0.96 |
| | K_S (L/ μ g) | 3.56×10^{-5} | 5.83×10^{-5} |
| | $q_m (mg/g)$ | 3045 | 12,133 |
| | n | 1.32 | 1.20 |

exhibited much higher maximum adsorption capacity than those of reported biosorbents. Additionally, compared with those reported, our aerogels had at least four unique features: 1) in addition to PFOA and PFOS commonly studied at mg/L levels by other researchers, our two aerogels had superior sorption of a mixture of PFASs at the low end of µg/L levels that is environmentally relevant. Since PFASs often show up in contaminated environments as mixtures (Gagliano et al., 2020), our aerogels hold high promise to remediate environments containing mixed PFASs at low concentrations (Ateia et al., 2019); 2) theoretically, long chain PFASs, due to their stronger binding with a sorbent, outcompete short chains and lead to desorption of short chain PFAS over time (McCleaf et al., 2017). In this study, although short chain PFASs were not 100% removed, the adsorption increased with time and desorption was not observed to occur at least within the tested duration of 24 h; 3) the adsorption of relatively hydrophobic PFASs appeared to be spontaneous. The short contact time will allow fast throughput and rapid treatment of PFASs contaminated water; and 4) the aerogels retaining their shape and structure integrity after PFASs sorption can be easily and completely separated from aqueous solutions. This eliminates the need of centrifugation or filtration for separating powdered sorbents from water. (Li et al., 2022)., (Zhang et al., 2019)

4. Future perspectives

The ALGPEI-3 and GTH-CTNPEI aerogels' extremely high sorption capacities and unique features as being green, sustainable, independent of pH, and easily separable from aqueous solutions warrant their further investigations. To truly use these aerogels for removing PFASs in environmental water matrices, at least four aspects, such as regenerability and reuse; final disposal of the spent sorbents; the aerogels' selectivity toward PFAS in real contaminated water; and the overall economic and environmental impacts must be considered. In addition, further surface modifications of CTN and ALG are needed to increase their affinity toward capturing short and ultrashort chain PFAAs; cationic, and zwitterionic PFASs. Furthermore, it is necessary to investigate the sorption mechanisms from the molecular interaction's perspective, such as sorption location and binding energy of the PFASs with that of aerogels' surface using different tools, for example, X-ray photoelectron spectroscopy (XPS) analysis (Ordonez et al., 2022) (Liu et al., 2022), and density functional theory (DFT) model (Liu et al., 2022), (Yan et al., 2020b). Moreover, the shape recovery (mechanical performance) of the aerogels needs to be identified using compressive stress-strain studies (Wang et al., 2022).

5. Conclusions

To the best of our knowledge, this is the first study screening a total of 11 bio-based fibers/aerogels for adsorption of a mixture of 12 PFASs at environmentally relevant concentrations in water. Out of the 11 biosorbents, ALGPEI-3 and GTH-CTNPEI aerogels were found to possess the highest sorption capacity for both short/long chain PFASs and precursor compounds. For both aerogels, although electrostatic interactions played a role, the dominant mechanism underlying PFASs sorption was hydrophobic interactions. This enables the aerogels' robustness in removing PFASs at a wide range of pH conditions. The spontaneous sorption of relatively hydrophobic PFASs, the structural stability of both aerogels under extreme pH, and the simple separation of aerogels from water point to potentially wide applications of these aerogels for removing PFASs in complex aqueous streams.

Author credit statement

Ilango Aswin Kumar: Conceptualization, Investigation, Data curation, Methodology, Resources, Software, Writing - Original draft, Writing - Review & editing Tao Jiang: Software, Writing - Review & editing Weilan Zhang: Writing - Review & editing Jeremy I. Feldblyum:

Writing - Review & editing Haralabos Efstathiadis: Writing - Review & editing Yanna Liang: Supervision, Investigation, Funding acquisition, Project Administration, Resources, Writing - Review & editing.

Declaration of competing interest

The authors declare that they have no known competing financial interests or personal relationships that could have appeared to influence the work reported in this paper.

Data availability

Data will be made available on request.

Acknowledgements

The authors acknowledge financial support from the U.S. National Science Foundation under award number CBET 2225596. We are also grateful to Kevin Shah from SUNY Polytechnic Institute for his assistance with SEM-EDS measurements, and to Crom Audrey from UAlbany for BET analyses.

Appendix A. Supplementary data

Supplementary data to this article can be found online at https://doi.org/10.1016/j.envpol.2023.121865.

References

- Ahmad, M., Manzoor, K., Chaudhuri, R.R., Ikram, S., 2017. Thiocarbohydrazide crosslinked oxidized chitosan and poly (vinyl alcohol): a green framework as efficient Cu (II), Pb (II), and Hg (II) adsorbent. J. Chem. Eng. Data 62, 2044–2055.
- Appleman, T.D., Higgins, C.P., Quinones, O., Vanderford, B.J., Kolstad, C., Zeigler-Holady, J.C., Dickenson, E.R., 2014. Treatment of poly-and perfluoroalkyl substances in US full-scale water treatment systems. Water Res. 51, 246–255.
- Arvaniti, O.S., Stasinakis, A.S., 2015. Review on the occurrence, fate and removal of perfluorinated compounds during wastewater treatment. Sci. Total Environ. 524, 81–92.
- Ateia, M., Alsbaiee, A., Karanfil, T., Dichtel, W., 2019. Efficient PFAS removal by amine-functionalized sorbents: critical review of the current literature. Environ. Sci. Technol. Lett. 6, 688–695.
- Ateia, M., Attia, M.F., Maroli, A., Tharayil, N., Alexis, F., Whitehead, D.C., Karanfil, T., 2018. Rapid removal of poly- and perfluorinated alkyl substances by poly (ethylenimine)-functionalized cellulose microcrystals at environmentally relevant conditions. Environ. Sci. Technol. Lett. 5, 764–769.
- Bao, S., Yang, W., Wang, Y., Yu, Y., Sun, Y., Li, K., 2020. PEI grafted amino-functionalized graphene oxide nanosheets for ultrafast and high selectivity removal of Cr (VI) from aqueous solutions by adsorption combined with reduction: behaviors and mechanisms. Chem. Eng. J. 399, 125762.
- Bazri, M.M., Mohseni, M., 2016. Impact of natural organic matter properties on the kinetics of suspended ion exchange process. Water Res. 91, 147–155.
- Bo, S., Luo, J., An, Q., Xiao, Z., Wang, H., Cai, W., Zhai, S., Li, Z., 2020. Efficiently selective adsorption of Pb (II) with functionalized alginate-based adsorbent in batch/column systems: mechanism and application simulation. J. Clean. Prod. 250, 110595
- Carter, K.E., Farrell, J., 2010. Removal of perfluorooctane and perfluorobutane sulfonate from water via carbon adsorption and ion exchange. Separ. Sci. Technol. 45, 762–767.
- Chen, W., Zhang, X., Mamadiev, M., Wang, Z., 2017. Sorption of perfluorooctane sulfonate and perfluorooctanoate on polyacrylonitrile fiber-derived activated carbon fibers: in comparison with activated carbon. RSC Adv. 7, 927–938.
- Ching, C., Klemes, M.J., Trang, B., Dichtel, W.R., Helbling, D.E., 2020. β-cyclodextrin polymers with different cross-linkers and ion-exchange resins exhibit variable adsorption of anionic, zwitterionic, and nonionic PFASs. Environ. Sci. Technol. 54, 12693–12702.
- Dangi, Y.R., Lin, X., Choi, J.-W., Lim, C.-R., Song, M.-H., Han, M., Bediako, J.K., Cho, C.-W., Yun, Y.-S., 2022. Polyethyleneimine functionalized alginate composite fiber for fast recovery of gold from acidic aqueous solutions. Environ. Technol. Innov. 28, 102605.
- Deng, S., Yu, Q., Huang, J., Yu, G., 2010. Removal of perfluorooctane sulfonate from wastewater by anion exchange resins: effects of resin properties and solution chemistry. Water Res. 44, 5188–5195.
- Dixit, F., Barbeau, B., Mostafavi, S.G., Mohseni, M., 2019. PFOA and PFOS removal by ion exchange for water reuse and drinking applications: role of organic matter characteristics. Environ. Sci. J. Integr. Environ. Res.: Water Research & Technology 5, 1782–1795.

- Du, Z., Deng, S., Chen, Y., Wang, B., Huang, J., Wang, Y., Yu, G., 2015. Removal of perfluorinated carboxylates from washing wastewater of perfluorooctanesulfonyl fluoride using activated carbons and resins. J. Hazard Mater. 286, 136–143.
- Feng, Y., Wang, H., Xu, J., Du, X., Cheng, X., Du, Z., Wang, H., 2021. Fabrication of MXene/PEI functionalized sodium alginate aerogel and its excellent adsorption behavior for Cr (VI) and Congo Red from aqueous solution. J. Hazard Mater. 416, 125777.
- Finnegan, C., Ryan, D., Enright, A.-M., Garcia-Cabellos, G., 2018. A review of strategies for the detection and remediation of organotin pollution. Crit. Rev. Environ. Sci. Technol. 48, 77–118.
- Gagliano, E., Sgroi, M., Falciglia, P.P., Vagliasindi, F.G., Roccaro, P., 2020. Removal of poly-and perfluoroalkyl substances (PFAS) from water by adsorption: role of PFAS chain length, effect of organic matter and challenges in adsorbent regeneration. Water Res. 171, 115381.
- Gong, Y., Wang, L., Liu, J., Tang, J., Zhao, D., 2016. Removal of aqueous perfluorooctanoic acid (PFOA) using starch-stabilized magnetite nanoparticles. Sci. Total Environ. 562, 191–200.
- Harris, J.T., de la Garza, G.D., Devlin, A.M., McNeil, A.J., 2022. Rapid removal of polyand perfluoroalkyl substances with quaternized wood pulp. ACS ES&T Water 2, 349,356
- Hassan, M., Du, J., Liu, Y., Naidu, R., Zhang, J., Ahsan, M.A., Qi, F., 2022. Magnetic biochar for removal of perfluorooctane sulphonate (PFOS): interfacial interaction and adsorption mechanism. Environ. Technol. Innov. 28, 102593.
- Higgins, C.P., Luthy, R.G., 2006. Sorption of perfluorinated surfactants on sediments. Environ. Sci. Technol. 40, 7251–7256.
- Jiang, T., Zhang, W., Ilango, A.K., Feldblyum, J.I., Wei, Z., Efstathiadis, H., Yigit, M.V., Liang, Y., 2022. Surfactant-modified clay for adsorption of mixtures of per- and polyfluoroalkyl substances (PFAS) in aqueous solutions. ACS Applied Engineering Materials.
- Jiang, T., Zhang, W., Ilango, A.K., Feldblyum, J.I., Wei, Z., Efstathiadis, H., Yigit, M.V., Liang, Y., 2023. Surfactant-modified clay for adsorption of mixtures of per- and polyfluoroalkyl substances (PFAS) in aqueous solutions. ACS Applied Engineering Materials 1, 394–407.
- Jiang, Y.-J., Yu, X.-Y., Luo, T., Jia, Y., Liu, J.-H., Huang, X.-J., 2013. γ-Fe2O3 nanoparticles encapsulated millimeter-sized magnetic chitosan beads for removal of Cr (VI) from water: thermodynamics, kinetics, regeneration, and uptake mechanisms. J. Chem. Eng. Data 58, 3142–3149.
- Karthik, R., Meenakshi, S., 2015. Removal of Pb (II) and Cd (II) ions from aqueous solution using polyaniline grafted chitosan. Chem. Eng. J. 263, 168–177.
- Kopac, T., Kırca, Y., Toprak, A., 2017. Synthesis and characterization of KOH/boron modified activated carbons from coal and their hydrogen sorption characteristics. Int. J. Hydrogen Energy 42, 23606–23616.
- Kumar, I.A., Naushad, M., Ahamad, T., Viswanathan, N., 2021. Development of triaminotriazine functionalized graphene oxide capped chitosan porous composite beads for nutrients remediation towards water purification. Int. J. Biol. Macromol. 170, 13–23.
- Kumar, I.A., Viswanathan, N., 2017. Fabrication of metal ions cross-linked alginate assisted biocomposite beads for selective phosphate removal. J. Environ. Chem. Eng. 5, 1438–1446.
- Kumar, I.A., Viswanathan, N., 2018. Hydrothermal fabrication of zirconium oxyhydroxide capped chitosan/kaolin framework for highly selective nitrate and phosphate retention. Ind. Eng. Chem. Res. 57, 14470–14481.
- Li, J., Li, X., Da, Y., Yu, J., Long, B., Zhang, P., Bakker, C., McCarl, B.A., Yuan, J.S., Dai, S. Y., 2022. Sustainable environmental remediation via biomimetic multifunctional lignocellulosic nano-framework. Nat. Commun. 13, 4368.
- Li, J., Zuo, K., Wu, W., Xu, Z., Yi, Y., Jing, Y., Dai, H., Fang, G., 2018. Shape memory aerogels from nanocellulose and polyethyleneimine as a novel adsorbent for removal of Cu (II) and Pb (II). Carbohydr. Polym. 196, 376–384.
- Liang, W., Wang, B., Cheng, J., Xiao, D., Xie, Z., Zhao, J., 2021. 3D, eco-friendly metalorganic frameworks@ carbon nanotube aerogels composite materials for removal of pesticides in water. J. Hazard Mater. 401, 123718.
- Lindstrom, A.B., Strynar, M.J., Libelo, E.L., 2011. Polyfluorinated compounds: past, present, and future. Environ. Sci. Technol. 45, 7954–7961.
- Liu, L., Li, Y., Coelhan, M., Chan, H.M., Ma, W., Liu, L., 2016. Relative developmental toxicity of short-chain chlorinated paraffins in Zebrafish (Danio rerio) embryos. Environ. Pollut. 219, 1122–1130.
- Liu, X., Zhu, C., Yin, J., Li, J., Zhang, Z., Li, J., Shui, F., You, Z., Shi, Z., Li, B., 2022. Installation of synergistic binding sites onto porous organic polymers for efficient removal of perfluorooctanoic acid. Nat. Commun. 13, 2132.
- Lü, T., Ma, R., Ke, K., Zhang, D., Qi, D., Zhao, H., 2021. Synthesis of gallic acid functionalized magnetic hydrogel beads for enhanced synergistic reduction and adsorption of aqueous chromium. Chem. Eng. J. 408, 127327.
- Lu, Y., Fan, L., Yang, L.-Y., Huang, F., Ouyang, X.-k., 2020. PEI-modified core-shell/bead-like amino silica enhanced poly (vinyl alcohol)/chitosan for diclofenac sodium efficient adsorption. Carbohydr. Polym. 229, 115459.
- Luft, C.M., Schutt, T.C., Shukla, M.K., 2022. Properties and mechanisms for PFAS adsorption to aqueous clay and humic soil components. Environ. Sci. Technol. 56, 10053–10061.
- McCleaf, P., Englund, S., Östlund, A., Lindegren, K., Wiberg, K., Ahrens, L., 2017. Removal efficiency of multiple poly-and perfluoroalkyl substances (PFASs) in drinking water using granular activated carbon (GAC) and anion exchange (AE) column tests. Water Res. 120, 77–87.
- Mo, L., Pang, H., Tan, Y., Zhang, S., Li, J., 2019. 3D multi-wall perforated nanocellulose-based polyethylenimine aerogels for ultrahigh efficient and reversible removal of Cu (II) ions from water. Chem. Eng. J. 378, 122157.

- Mukhopadhyay, R., Sarkar, B., Palansooriya, K.N., Dar, J.Y., Bolan, N.S., Parikh, S.J., Sonne, C., Ok, Y.S., 2021. Natural and engineered clays and clay minerals for the removal of poly-and perfluoroalkyl substances from water: state-of-the-art and future perspectives. Adv. Colloid Interface Sci. 297, 102537.
- Negahban, S.A.R., Ghorbani Shahna, F., Rahimpoor, R., Jalali, M., Rahiminejad, S., Soltanian, A., Bahram, A., 2014. Evaluating occupational exposure to carcinogenic volatile organic compounds in an oil-dependent chemical industry: a case study on benzen and epichlorohydrin. Journal of Occupational Hygiene Engineering 1, 36–46.
- Oladipo, A.A., Gazi, M., 2014. Enhanced removal of crystal violet by low cost alginate/ acid activated bentonite composite beads: optimization and modelling using nonlinear regression technique. J. Water Proc. Eng. 2, 43–52.
- Pan, J., Li, Y., Chen, K., Zhang, Y., Zhang, H., 2021. Enhanced physical and antimicrobial properties of alginate/chitosan composite aerogels based on electrostatic interactions and noncovalent crosslinking. Carbohydr. Polym. 266, 118102.
- Pandi, K., Viswanathan, N., 2015. Enhanced defluoridation and facile separation of magnetic nano-hydroxyapatite/alginate composite. Int. J. Biol. Macromol. 80, 341–349.
- Rabinow, L., 2022. Parts Per Trillion.
- Rahman, M.F., Peldszus, S., Anderson, W.B., 2014. Behaviour and fate of perfluoroalkyl and polyfluoroalkyl substances (PFASs) in drinking water treatment: a review. Water Res. 50, 318–340.
- Saha, D., Khan, S., Van Bramer, S.E., 2021. Can porous carbons be a remedy for PFAS pollution in water? A perspective. J. Environ. Chem. Eng. 9, 106665.
- Saleh, N.B., Khalid, A., Tian, Y., Ayres, C., Sabaraya, I.V., Pietari, J., Hanigan, D., Chowdhury, I., Apul, O.G., 2019. Removal of poly-and per-fluoroalkyl substances from aqueous systems by nano-enabled water treatment strategies. Environ. Sci. J. Integr. Environ. Res.: Water Research & Technology 5, 198–208.
- Shan, C., Wang, L., Li, Z., Zhong, X., Hou, Y., Zhang, L., Shi, F., 2019. Graphene oxide enhanced polyacrylamide-alginate aerogels catalysts. Carbohydr. Polym. 203, 19–25.
- Stratton, G.R., Dai, F., Bellona, C.L., Holsen, T.M., Dickenson, E.R., Mededovic Thagard, S., 2017. Plasma-based water treatment: efficient transformation of perfluoroalkyl substances in prepared solutions and contaminated groundwater. Environ. Sci. Technol. 51, 1643–1648.
- Tan, W., Zhang, Y., Szeto, Y.-s., Liao, L., 2008. A novel method to prepare chitosan/ montmorillonite nanocomposites in the presence of hydroxy-aluminum oligomeric cations. Compos. Sci. Technol. 68, 2917–2921.
- Tian, D., Geng, D., Mehler, W.T., Goss, G., Wang, T., Yang, S., Niu, Y., Zheng, Y., Zhang, Y., 2021. Removal of perfluorooctanoic acid (PFOA) from aqueous solution by amino-functionalized graphene oxide (AGO) aerogels: influencing factors, kinetics. isotherms. and thermodynamic studies. Sci. Total Environ. 783, 147041.
- Tzabar, N., ter Brake, H.J.M., 2016. Adsorption isotherms and Sips models of nitrogen, methane, ethane, and propane on commercial activated carbons and polyvinylidene chloride. Adsorption 22, 901–914.
- Waidyanatha, S., Gaudette, N.F., Hong, Y., Fennell, T.R., 2014. formation of epichlorohydrin, a known rodent carcinogen, following oral administration of 1,3-Dichloro-2-propanol in rats. Chem. Res. Toxicol. 27, 1787–1795.
- Wang, M., Orr, A.A., Jakubowski, J.M., Bird, K.E., Casey, C.M., Hearon, S.E., Tamamis, P., Phillips, T.D., 2021a. Enhanced adsorption of per-and polyfluoroalkyl substances (PFAS) by edible, nutrient-amended montmorillonite clays. Water Res. 188. 116534.
- Wang, Q., Li, L., Tian, Y., Kong, L., Cai, G., Zhang, H., Zhang, J., Zuo, W., Wen, B., 2022. Shapeable amino-functionalized sodium alginate aerogel for high-performance adsorption of Cr (VI) and Cd (II): experimental and theoretical investigations. Chem. Eng. J. 446, 137430.
- Wang, Q., Tian, Y., Kong, L., Zhang, J., Zuo, W., Li, Y., Cai, G., 2021b. A novel 3D superelastic polyethyleneimine functionalized chitosan aerogels for selective

- removal of Cr(VI) from aqueous solution: performance and mechanisms. Chem. Eng. J. 425, 131722.
- Wang, W., Maimaiti, A., Shi, H., Wu, R., Wang, R., Li, Z., Qi, D., Yu, G., Deng, S., 2019.
 Adsorption behavior and mechanism of emerging perfluoro-2-propoxypropanoic acid (GenX) on activated carbons and resins. Chem. Eng. J. 364, 132–138.
- Wawrzkiewicz, M., Hubicki, Z., 2009. Removal of tartrazine from aqueous solutions by strongly basic polystyrene anion exchange resins. J. Hazard Mater. 164, 502–509
- Xiao, F., Davidsavor, K.J., Park, S., Nakayama, M., Phillips, B.R., 2012. Batch and column study: sorption of perfluorinated surfactants from water and cosolvent systems by Amberlite XAD resins. J. Colloid Interface Sci. 368, 505–511.
- Yan, B., Munoz, G., Sauvé, S., Liu, J., 2020a. Molecular mechanisms of per- and polyfluoroalkyl substances on a modified clay: a combined experimental and molecular simulation study. Water Res. 184, 116166.
- Yan, B., Munoz, G., Sauvé, S., Liu, J., 2020b. Molecular mechanisms of per-and polyfluoroalkyl substances on a modified clay: a combined experimental and molecular simulation study. Water Res. 184, 116166.
- Yan, Y.-Z., An, Q.-D., Xiao, Z.-Y., Zhai, S.-R., Zhai, B., Shi, Z., 2017a. Interior multi-cavity/surface engineering of alginate hydrogels with polyethylenimine for highly efficient chromium removal in batch and continuous aqueous systems. J. Mater. Chem. 5, 17073–17087.
- Yan, Y., An, Q., Xiao, Z., Zheng, W., Zhai, S., 2017b. Flexible core-shell/bead-like alginate@ PEI with exceptional adsorption capacity, recycling performance toward batch and column sorption of Cr (VI). Chem. Eng. J. 313, 475–486.
- Yan, Y., Wang, Y., Wu, J., Wang, Z., Shen, X., Sun, Q., Jin, C., 2019. Preparation and characterization of high-strength and water resistant lignocelluloses based composites bonded by branched polyethylenimine (PEI). Int. J. Biol. Macromol. 141, 369–377.
- Yang, A., Ching, C., Easler, M., Helbling, D.E., Dichtel, W.R., 2020. Cyclodextrin polymers with nitrogen-containing tripodal crosslinkers for efficient PFAS adsorption. ACS Materials Letters 2, 1240–1245.
- Yao, Y., Volchek, K., Brown, C.E., Robinson, A., Obal, T., 2014. Comparative study on adsorption of perfluorooctane sulfonate (PFOS) and perfluorooctanoate (PFOA) by different adsorbents in water. Water Sci. Technol. 70, 1983–1991.
- Zaggia, A., Conte, L., Falletti, L., Fant, M., Chiorboli, A., 2016. Use of strong anion exchange resins for the removal of perfluoroalkylated substances from contaminated drinking water in batch and continuous pilot plants. Water Res. 91, 137–146.
- Zhang, D., He, Q., Wang, M., Zhang, W., Liang, Y., 2021. Sorption of perfluoroalkylated substances (PFASs) onto granular activated carbon and biochar. Environ. Technol. 42, 1798–1809.
- Zhang, D.Q., Zhang, W.L., Liang, Y.N., 2019. Adsorption of perfluoroalkyl and polyfluoroalkyl substances (PFASs) from aqueous solution - a review. Sci. Total Environ. 694. 133606.
- Zhang, H., Xiao, R., Li, R., Ali, A., Chen, A., Zhang, Z., 2020. Enhanced aqueous Cr (VI) removal using chitosan-modified magnetic biochars derived from bamboo residues. Chemosphere 261, 127694.
- Zhang, K., Huang, J., Yu, G., Zhang, Q., Deng, S., Wang, B., 2013. Destruction of perfluorooctane sulfonate (PFOS) and perfluorooctanoic acid (PFOA) by ball milling. Environ. Sci. Technol. 47, 6471–6477.
- Zhao, Q., Zhu, X., Chen, B., 2018. Stable graphene oxide/poly (ethyleneimine) 3D aerogel with tunable surface charge for high performance selective removal of ionic dyes from water. Chem. Eng. J. 334, 1119–1127.
- Zhou, Q., Deng, S., Yu, Q., Zhang, Q., Yu, G., Huang, J., He, H., 2010. Sorption of perfluorooctane sulfonate on organo-montmorillonites. Chemosphere 78, 688–694.
- Zhou, Z., Lin, S., Yue, T., Lee, T.-C., 2014. Adsorption of food dyes from aqueous solution by glutaraldehyde cross-linked magnetic chitosan nanoparticles. J. Food Eng. 126, 133–141